Design and measurement of a thin and light absorbing for space applications

Yenni Pinto, Julien Sarrazin, Anne Claire Lepage, Xavier Begaud, Nicolas Capet

Appl. Phys. A (2014) 115:541–545
DOI 10.1007/s00339-013-8097-1

Applied Physics A
Materials Science & Processing

Design and measurement of a thin and light absorbing material for space applications

Yenny Pinto · Julien Sarrazin · Anne Claire Lepage · Xavier Begaud · Nicolas Capet

Received: 15 October 2013/ Accepted: 15 October 2013 / Published online: 5 November 2013

Abstract This paper presents the design, realization and measurement of a thin lightweight absorbing material for space applications. Absorber design is based on high impedance surfaces loaded with resistors and known as a resistive high impedance surface (RHIS). The behavior of RHIS is analyzed at normal and oblique incidences for TE and TM polarizations. Prototypes have been realized and measured. Final design has a reflection coefficient less than −15 dB in S-Band (2–2.3 GHz) at normal incidence and till an angular dispersion of 40° for waves in TE polarization, and 35° for waves in TM polarization. Simulation results are validated by measurement.

1 Introduction

Absorbing material can be used to reduce the reflection of electromagnetic waves on a surface. For space applications, these materials may for example be placed on the satellite to reduce interference between antennas. Conventional design methods consist in the insertion of losses on the surface of the material. The Salisbury screen [1] is an example of this approach in which a resistive layer is placed on top of a metal surface at a distance equal to a quarter wavelength. The major drawback of this resonant structure is to operate on a narrow band of frequencies. The Jauman absorber [2], consisting of several resistive layers spaced approximately by a quarter wavelength, operates over a wide band. However, this technique greatly increases the thickness of the structure.

In 2002, Engheta proposed to introduce metamaterials in the design of absorbers [3]. This approach has represented a technological breakthrough as it allows reducing drastically the thickness. Thus, in [4] the use of a high impedance surface (HIS) associated with a resistive material as absorber is presented. This type of structure, called resistive high impedance surface (RHIS), consists of a frequency selective surface (FSS) over a grounded dielectric slab. The FSS is usually a periodic array of printed patterns loaded with resistors or resistive sheets to achieve absorption. Such a material has the advantage of being lightweight and thin.

In this article, RHIS is optimized for good absorption performance (magnitude of the reflection coefficient $|\Gamma| < -15$ dB) in the band (2–2.3 GHz) (14 %) at normal incidence, while fulfilling specific constraints for space applications as a low mass density (<2.5 kg/m^2) and a thickness less than 50 mm. This structure is also analyzed at oblique incidence for TE and TM polarizations.

The paper is organized as follows: in the next Section, the design of the RHIS structure is described, in Sect. 3, the experimental validation and results are presented, and finally in Sect. 4, conclusions are given.

2 RHIS design

The RHIS structure is composed of square patches interconnected by resistors on top of a grounded dielectric slab. Figure 1 shows the unit cell of the RHIS structure. It is composed of square copper patches over Rogers RO4003 substrate ($\varepsilon_r = 3.38 \pm 0.05$). Below, are a honeycomb layer ($\varepsilon_r = 1.08 \pm 0.05$) and the ground plane, consisting of a copper film. Interconnecting patches, resistors are formed with TICER

Y. Pinto (✉) · A. C. Lepage · X. Begaud
Institut Mines-Télécom, Télécom ParisTech, Paris, France
e-mail: pintobal@telecom-paristech.fr

J. Sarrazin
UMPC Univ. Paris 06, UR2, L2E, Paris, France

N. Capet
Centre National d'Etudes Spatiales, Toulouse, France

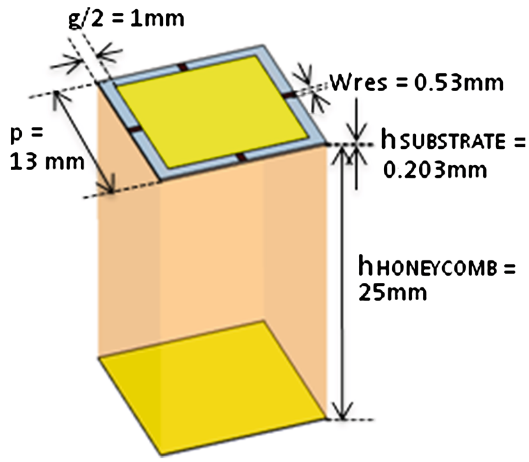

Fig. 1 Unit cell of RHIS

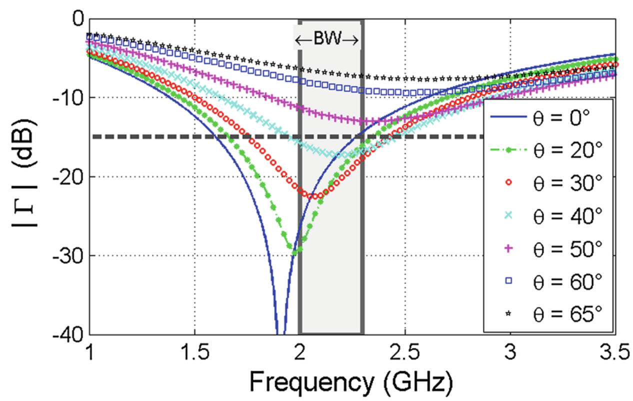

Fig. 2 Simulated reflection coefficient at normal and oblique incidence. TE polarization (*BW* required bandwidth)

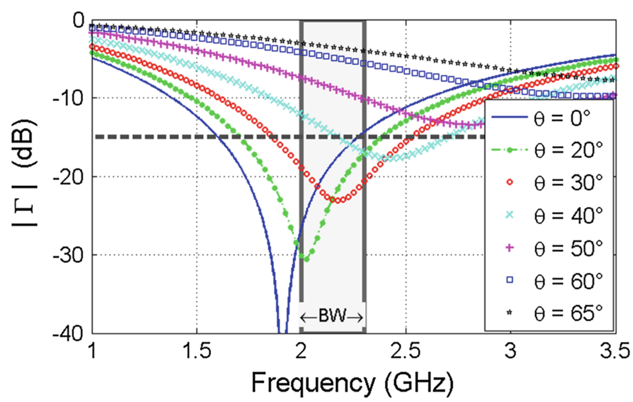

Fig. 3 Simulated reflection coefficient at normal and oblique incidence. TM polarization (*BW* required bandwidth)

resistive film with width $W_{res} = 0.53$ mm, resistivity 100 Ω/square and thickness $t = 0.1\,\mu$m which provides a resistance of 377 Ω.

The structure is simulated and optimized using the CST Microwave Studio (frequency solver) [5]. For simulations, only one cell is considered and periodical boundaries are applied.

2.1 Simulation results

The structure is optimized to obtain a reflection coefficient lower than −15 dB ($|\Gamma| < -15$ dB) in a wider band [(1.6–2.3 GHz) 36 %] than required [(2–2.3 GHz) 14 %] for normal incidence, to compensate, to some extent, the expected performance degradation when the incidence angle increases. This structure is also analyzed at oblique incidence for TE and TM polarizations. The simulations results are given in Figs. 2 and 3. A good absorption performance ($|\Gamma| < -15$ dB) in the targeted band (2–2.3 GHz) is observed at normal incidence for both polarizations. When the angular dispersion increases, the absorption level decreases and the frequency band shifts. Consequently, a reflection coefficient lower than −15 dB in the 2–2.3 GHz band is limited to an angular dispersion of 40° for waves in TE polarization, and 35° for waves in TM polarization.

3 Experimental validation

3.1 Prototype

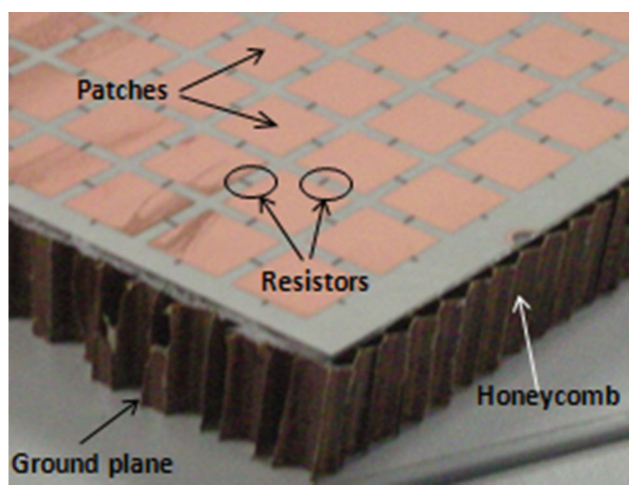

Fig. 4 Prototype

Figure 4 shows the prototype. It is composed of three layers. The first one is a Rogers RO4003 substrate with the patches and the resistive sheet (TICER 100 Ω/square) above it. This layer has a thickness of 0.203 mm. The second layer consists in a honeycomb with a 25-mm thickness, and the third one is the ground plane (a copper sheet of 35 μm). All the layers are added together using double-sided adhesive film. The total thickness of the structure is about 25.3 mm (∼0.17 λ at 2.1 GHz), thereby meeting the specifications.

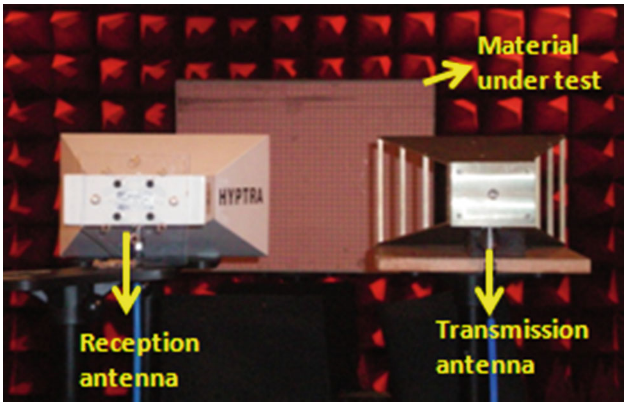

Fig. 5 Measurement setup at normal incidence

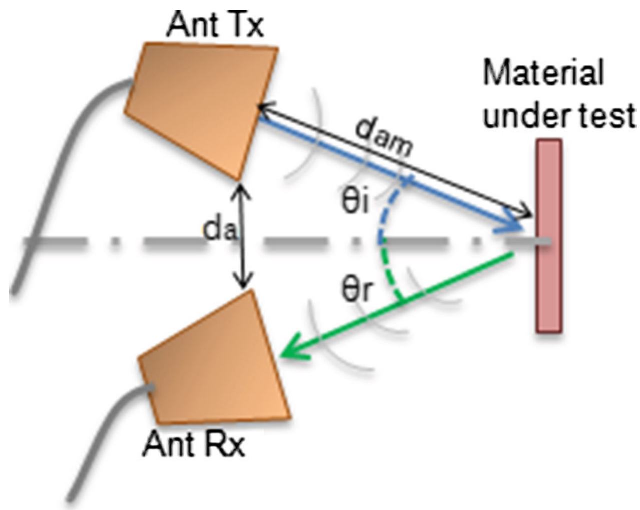

Fig. 6 Measurement setup at oblique incidence

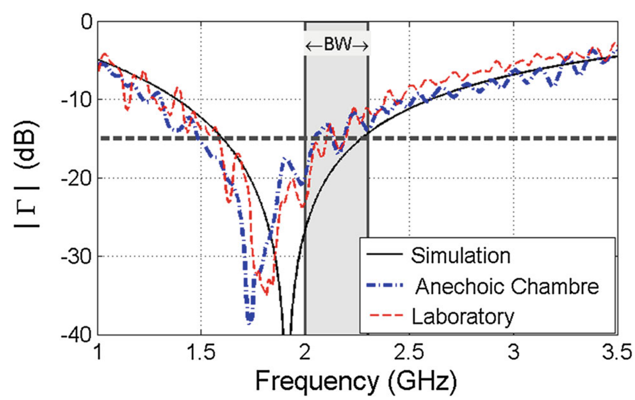

Fig. 7 Comparison between simulation and measurements results at normal incidence (d_a= 8 cm, d_{am} =107 cm)

The total size of the prototype is 578 × 428 mm and the mass density is about 2.4 kg/m^2.

3.2 Measurement setup

The measurement of the reflection coefficient of the absorbing material is carried out in three stages:

- Measurement with a reference metallic plane (Γ_{PEC})
- Measurement with the RHIS structure (Γ_{RHIS})
- Calculation of the reflection coefficient of material under test using (1).

$$|\Gamma| = \frac{|\Gamma\_{RHIS}|}{|\Gamma\_{PEC}|}, \tag{1}$$

The reflection coefficient is measured using two horn antennas. These are positioned in front of the material under test (MUT). The two horn antennas are connected to a network analyzer E5071C Agilent. The measurement setup at normal incidence is shown in Fig. 5.

The antennas are positioned (Fig. 6) at a distance (d_{am}) of MUT and are separated by a distance (d_a). The material is positioned at a height of 1.15 m above the ground.

The Figure 6 illustrates the measurement setup at oblique incidence. The distance between the antenna and MUT is d_{am} = 107 cm. MUT is fixed and the antennas are displaced according to incidence angle ($\theta_i = \theta_r$).

3.3 Measurement results

Measurements were realized in two different environments. The first environment is an anechoic chamber where the conditions are suitable to eliminate external interferences and absorb reflections of electromagnetic waves. Second measurements are realized in a laboratory without ideal conditions. The objective is then to estimate if the RHIS structure is efficient in a perturbed environment like a laboratory. The Fig. 7 shows results at normal incidence comparing the measurements from two different environments and simulation. A good agreement between results is obtained, however, a shift in frequency band is observed between simulation and measurements. The influence of the environment is noticeable. Indeed, measurement in laboratory presents more oscillations than measurements in anechoic chamber.

To explain the oscillations presence in both laboratory and anechoic chamber results, different measurements in anechoic chamber, where the distance between antennas and material is changed are performed. First, the distance (d_{am}) is changed from near field (d_{am}= 35 cm) to far field (d_{am} = 130 cm). The results are displayed in Fig. 8. Differences in absorption levels are observed when measurements are realized in the near field. For all cases, the percentage of the frequency shift (according to simulation result) is about 10 %. The oscillations are present in all cases.

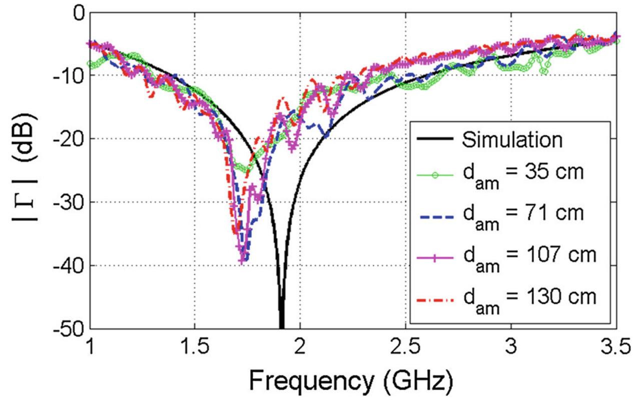

Fig. 8 Influence of the measurement distance (d_{am}) on the reflection coefficient (normal incidence, $d_a = 8$ cm)

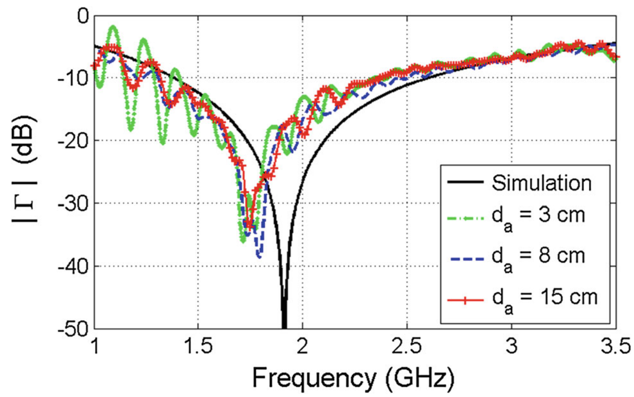

Fig. 9 Influence of the distance between Tx and Rx Antennas (d_a) on the reflection coefficient (at normal incidence and with $d_{am} = 107$ cm)

Then, the influence of the separating distance between the antennas (d_a) is shown in Fig. 9.

The oscillations amplitude increases when the value of d_a decreases. Thus the coupling between the antennas is probably the cause of the oscillations.

For oblique incidence, the measurements are performed for angles 45° and 60°. The results are plotted in Figs. 10 and 11 for TE polarization. All the following measurements have been realized in the laboratory (Figs. 10, 11, 12 and 13) with $d_{am} = 107$ cm. There is an agreement, but differences in frequency and level are observed. At oblique incidence for 45° and 60°, requirements are not reached. In fact, after 35°, the bandwidth shifts to low frequencies and the level increases.

Measurements for TM polarization are presented in Figs. 12 and 13.

Shifts in frequency and level can be explained by different ways:

– The imperfections of realization.
– The simulation does not take into account the presence of the double-sided adhesive film.

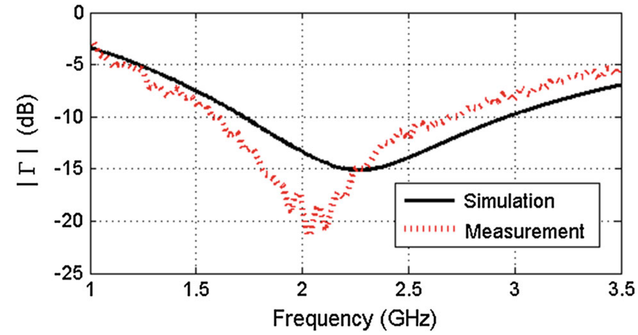

Fig. 10 Comparison between simulation and measurements results at oblique incidence (45°). TE polarization

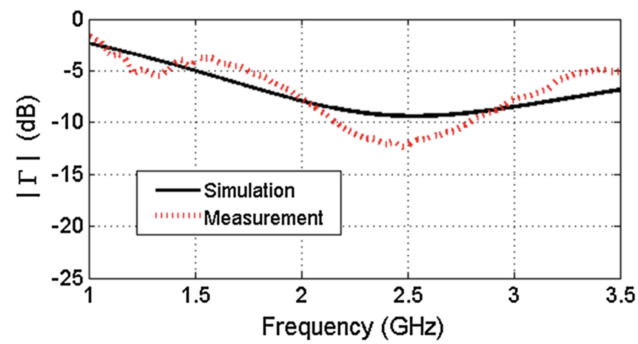

Fig. 11 Comparison between simulation and measurements results at oblique incidence (60°). TE polarization

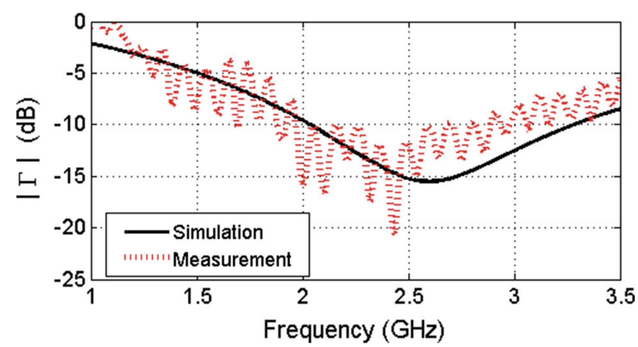

Fig. 12 Comparison between simulation and measurements results at oblique incidence (45°). TM polarization

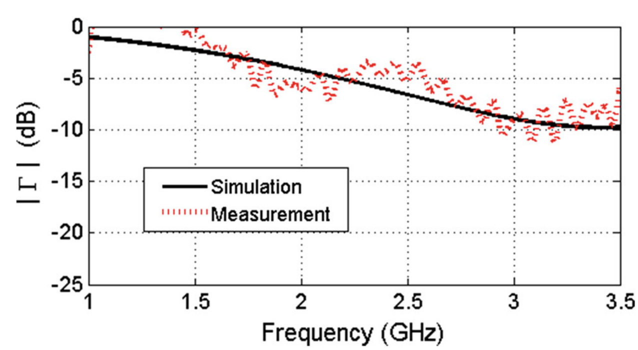

Fig. 13 Comparison between simulation and measurements results at oblique incidence (60°). TM polarization

– The resistance value is not accurate and has a tolerance of ±10 %.
– The permittivity value of honeycomb is not accurate.

4 Conclusion

The design, realization and measurement of a thin lightweight absorbing material for space applications have been presented. Absorber design is based on HIS loaded with resistors and known as a RHIS. The behavior of RHIS has been analyzed at normal and oblique incidences for TE and TM polarizations. Simulation results have been compared to measurement. Measurements were realized in two different environments: anechoic chamber and laboratory. There is a good agreement, despite some differences in frequency and level. Shifts in frequency and level can be explained by the imperfections of realization, tolerances of materials and the adhesive film not taken into account in the simulation. Further investigation will be driven to highlight and reduce all these uncertainties.

Final design has a reflection coefficient less than −15 dB in S-Band (2–2.3 GHz) at normal incidence and till an angular dispersion of 40° for waves in TE polarization, and 35° for waves in TM polarization.

References

1. W.W. Salisbury, Absorbent body for electromagnetic waves, U.S. Patent 2599944, June 1952.
2. L.J. Du Toit, The design of Jauman absorbers. IEEE Antennas Propag. Mag. **36**(6), 17–25 (1994)
3. N. Engheta, Thin absorbing screens using metamaterial surfaces. IEEE Antennas Propag. Symp. **2**, 392–395 (2002)
4. F. Costa, A. Monorchio, G. Manara, Analysis and design of ultra thin electromagnetic absorbers comprising resistively loaded high impedance surfaces. IEEE Trans. Antennas Propag. **58**(5), 1551–1558 (2010)
5. F. Linot, X. Begaud, M. Soiron, C. Renard, M. Labeyrie, Characterization of a loaded high impedance surface. Int. J. Microw. Wirel. Technol. **1**, 483–487 (2009)